

# Band gap modified Al-doped $\text{Zn}_{1-x}\text{Mg}_x\text{O}$ and $\text{Zn}_{1-y}\text{Cd}_y\text{O}$ transparent conducting thin films

L. B. Duan · X. R. Zhao · J. M. Liu ·  
W. C. Geng · H. N. Sun · H. Y. Xie

Received: 23 August 2011 / Accepted: 3 October 2011 / Published online: 13 October 2011  
© Springer Science+Business Media, LLC 2011

**Abstract** Al-doped  $\text{Zn}_{1-x}\text{Mg}_x\text{O}$  and  $\text{Zn}_{1-y}\text{Cd}_y\text{O}$  thin films were prepared on glass substrates by sol–gel method. The codoping thin films showed preferential *c*-axis orientation, and the lattice constant *c* evaluated from the shift of the position of (002) peak displayed an increasing evolution from  $x = 8$  at.% to  $y = 8$  at.%, indicating a roughly statistical substitution of  $\text{Mg}^{2+}$  and  $\text{Cd}^{2+}$  for  $\text{Zn}^{2+}$  in their solid solution. The effects of narrowing and widening band gap ( $E_g$ ) on conductivity of (Cd, Al) and (Mg, Al) codoped ZnO thin films were simultaneously investigated using transmission spectra and electrical measurements. The transmittances of these films are obviously decreased by vacuum annealing to 50–60%. However, the carrier concentration and Hall mobility both increase, and resistivity decreases with narrowing band gap in 1 at.% Al-doped  $\text{Zn}_{1-x}\text{Mg}_x\text{O}$  and  $\text{Zn}_{1-y}\text{Cd}_y\text{O}$  thin films from  $x = 8$  at.% to  $y = 8$  at.%. It is revealed that the conductivity of Al-doped ZnO thin films could be enhanced by this simple band gap modification.

## 1 Introduction

Transparent conducting oxide (TCO) is characterized by a unique combination of low electrical resistivity and high optical transparency. Tin-doped indium oxide (ITO) is a widely used material for TCO applications, such as flat panel displays and solar cells. However, indium is rare and expensive and its supply may be limited by the availability

of natural resources. ZnO is one of the most promising candidates for replacing ITO, because Zn is an abundant material and ZnO is a native *n*-type semiconductor with a band gap ( $E_g$ ) of 3.36 eV [1, 2]. To improve the conductivity, ZnO is typically doped with charged electron donors such as Al, Ga, In, etc. [3–5] Al-doped ZnO (ZAO) film resistivity of less than  $2 \times 10^{-4} \Omega \text{ cm}$  has been attained, which is comparable to those obtained in ITO films [3]. Furthermore, many investigators have examined the electrical and optical properties of Al-doped ZnO with a broad range of nominal Al-doping, and a critical Al content with the minimum resistivity is usually observed, depending on preparation methods and conditions [6–9]. Lu et al. [7] reported that the optimal result for ZAO films synthesized by magnetron sputtering located at Al content of 4%. Nasr et al. [9]. revealed that the minimum resistivity was obtained around 1.5–2% Al-doped ZnO films prepared by sol–gel method, and above the critical concentration, the segregated Al started to dominate the electrical transport.

In addition, the band gap of ZnO ( $E_g = 3.36$  eV) can be tuned by alloying with bivalent Mg or Cd. While Mg is known to enhance the band gap, Cd substitution leads to reduce in band gap, the resultant (Zn, Cd)O and (Zn, Mg)O alloys have allowed to cover a wide band gap range [10–12]. Actually, the thermodynamic solubility limits of MgO and CdO in MgO–ZnO and CdO–ZnO alloy systems are only about 4% [13] and 2% [10], respectively. In spite of the predicted low solubility, Ohtomo et al. [14] prepared solid solution  $\text{Mg}_x\text{Zn}_{1-x}\text{O}$  films with Mg content up to a value of  $x = 0.33$  by pulsed laser deposition (PLD) under metastable conditions. Above  $x = 33\%$ , MgO was reported to segregate from the wurtzite  $\text{MgZnO}$  lattice limiting its maximum band gap of 3.9 eV. Metal organic vapor phase epitaxy (MOVPE) was also employed by Park et al. [15] to grow high quality  $\text{Mg}_x\text{Zn}_{1-x}\text{O}$  films up to  $x = 0.49$  with

L. B. Duan (✉) · X. R. Zhao · J. M. Liu ·  
W. C. Geng · H. N. Sun · H. Y. Xie  
Key Laboratory of Space Applied Physics and Chemistry,  
Ministry of Education of China and School of Science,  
Northwestern Polytechnical University, 710072 Xi'an,  
People's Republic of China  
e-mail: lbduan@nwpu.edu.cn

the near-band-edge emission peak at 4.05 eV, while Ghosh et al. [16] reported the solubility limit of MgO in sol–gel  $\text{Mg}_x\text{Zn}_{1-x}\text{O}$  thin films lies in the composition range of  $0.05 < x < 0.08$ . Meanwhile, there also have been many reports on  $\text{Cd}_x\text{Zn}_{1-x}\text{O}$  film preparation by molecular beam epitaxy (MBE) [17], PLD [18], and MOVPE [19, 20]. The maximum content of cadmium in the wurtzite  $\text{Cd}_x\text{Zn}_{1-x}\text{O}$  is 0.085 from above research reports, while the crystal structure of  $\text{Cd}_x\text{Zn}_{1-x}\text{O}$  films grown by Ishihara et al. [21] using remote-plasma-enhanced MOVPE changed from wurtzite structure to rocksalt structure around  $x = 0.7$ , and the photoluminescence spectra were observed from the wurtzite  $\text{Cd}_x\text{Zn}_{1-x}\text{O}$  films in the range of 3.3–1.8 eV with  $x \leq 0.69$  at room temperature. A ZnO-based TCO with modified band gap gives rise to many of its scientific and technical applications, such as improving the efficiency of different wavelength light emitting devices when used as a transparent electrode [2, 13, 22]. Matsubara et al. [2] synthesized Al-doped  $\text{Zn}_{1-x}\text{Mg}_x\text{O}$  transparent conducting films by a PLD system, although film resistivity was found to increase with increasing Mg composition. Similarly, in  $\text{Zn}_{1-x}\text{Mg}_x\text{O}$  with 0.5 at.% Ga, resistivity also increased with increasing Mg concentration, and the carrier concentration and Hall mobility values were decreased in films with higher Mg content [23]. Therefore, it is a significant challenge to obtain band gap modified TCO without sacrificing the conductivity. Meanwhile, the simultaneous comparison of effects of narrowing and widening band gap by Cd or Mg codoping on conductivity of ZnO-based TCO has been rarely reported.

Numerous deposition methods have been applied to prepare highly conductive and transparent ZnO-based thin films, including chemical vapor deposition (CVD), MBE, PLD, magnetron sputtering, etc. [7, 24]. However, the industrial production is limited due to the complex and expensive vacuum technique. Furthermore, the preparation of homogeneous and large-area films is also an upfront challenge. The sol–gel method is a kind of cost-effective process and is helpful to realize the preparation of large-area homogeneous films [25]. More importantly, sol–gel method has the distinct advantages in excellent composition control and the ability to achieve atomic scale mixing of individual components [26]. In this work, we prepare the 1 at.% Al-doped  $\text{Zn}_{1-x}\text{Mg}_x\text{O}$  and  $\text{Zn}_{1-y}\text{Cd}_y\text{O}$  ( $x, y = 0–8$  at.%) thin films by sol–gel method to simultaneously investigate the effects of narrowing and widening band gap on the conductivity of Al-doped ZnO transparent conducting thin films.

## 2 Experimental procedure

Analytical grade zinc acetate [ $\text{Zn}(\text{CH}_3\text{COO})_2 \cdot 2\text{H}_2\text{O}$ ] was firstly dissolved in a 2-methoxyethanol ( $\text{C}_3\text{H}_8\text{O}_2$ ) and

monoethanolamine (MEA,  $\text{C}_2\text{H}_7\text{NO}$ ) solution at room temperature. The concentration of the sol was 0.75 mol/l and the molar ratio of MEA to zinc acetate was kept at 1.0. The solution was stirred at 60 °C for 1 h until it became clear and homogeneous. Aluminum nitrate [ $\text{Al}(\text{NO}_3)_3 \cdot 9\text{H}_2\text{O}$ ], magnesium nitrate [ $\text{Mg}(\text{NO}_3)_2 \cdot 6\text{H}_2\text{O}$ ], and cadmium nitrate [ $\text{Cd}(\text{NO}_3)_2 \cdot 4\text{H}_2\text{O}$ ] were added into some of the previous solutions in an appropriate ratio and then stirred vigorously at 60 °C for another 1 h. The final solutions served for coating were aged for 36 h at room temperature. The slice glass (Sail 7101, China) was used as substrate for sol–gel dip-coating after being cleaned in an ultrasonic bath for 15 min with HCl, ethanol and distilled water, respectively. The glass sheets were dipped into the aged solution for 1 min and then pulled out at the velocity of 4 cm/min. The films were kept at 100 °C in a drying box for 10 min and then preheated at 500 °C for 15 min. Such process was repeated for 10 times and then the films were annealed at 550 °C in air for 1 h before the final films were obtained. To improve the conductive properties, all the samples were treated by vacuum annealing ( $P \sim 10^{-2}$  Pa) instead.

X-ray diffraction (XRD) patterns were collected from 20° to 80° using PANalytical X'pert MPD PRO with Cu  $K_\alpha$  radiation. Optical properties such as transmittance were measured by UV–VIS spectrophotometer (Hitachi UV–VIS spectrophotometer U3010) in the wavelength of 300–800 nm. The thickness of the samples was carried out by spectroscopic ellipsometer (Spec EI-2000-VIS). The electrical properties such as resistivity, carrier concentration, and Hall mobility were detected by Hall effect measurements in the Van der Pauw configuration using a ET-9000 system at room temperature.

## 3 Results and discussion

Figure 1 displays the XRD patterns of 1 at.% Al-doped  $\text{Zn}_{1-x}\text{Mg}_x\text{O}$  and  $\text{Zn}_{1-y}\text{Cd}_y\text{O}$  ( $x, y = 0–8$  at.%) thin films treated by vacuum annealing. It shows that all the films have a single phase which can be identified as the hexagonal wurtzite structure of ZnO (space group  $P6_3mc$ ). No trace of other impurities is found within the detection limit of instrument. All the films show an extremely pronounced (002) texture with dominant peak  $2\theta \approx 34.4^\circ$ , indicating that the preferred orientation is along the crystallographic  $c$ -axis and perpendicular to the substrate. Since the effective ionic radius of  $\text{Zn}^{2+}$  (0.60 Å, coordination number CN = 4) is slightly larger than that of  $\text{Mg}^{2+}$  (0.57 Å, CN = 4), while evidently smaller than that of  $\text{Cd}^{2+}$  (0.78 Å, CN = 4), as showed in the inset of Fig. 1, the lattice constant  $c$  evaluated from the shift of the position of (002) peak shows an increasing evolution from  $x = 8\%$  to  $y = 8\%$ , indicating a roughly statistical

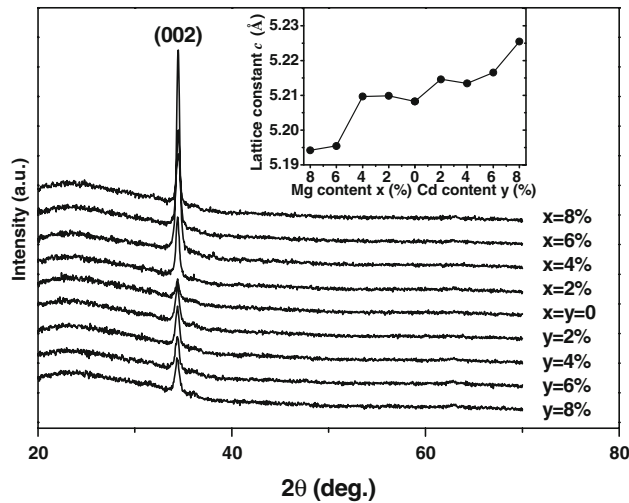


**Fig. 1** XRD patterns of 1 at.% Al-doped  $\text{Zn}_{1-x}\text{Mg}_x\text{O}$  and  $\text{Zn}_{1-y}\text{Cd}_y\text{O}$  ( $x, y = 0\text{--}8\%$  with an increment of 2 at.%) thin films. *Inset* the lattice constant  $c$  evaluated from the shift of the position of (002) peak

substitution of  $\text{Mg}^{2+}$  and  $\text{Cd}^{2+}$  for  $\text{Zn}^{2+}$  in their solid solution, although the unchanged lattice constant from  $x = 0$  to 4% for Mg doping, which might be due to the really close radius of  $\text{Mg}^{2+}$  and  $\text{Zn}^{2+}$  [10].

Actually, all 1 at.% Al-doped  $\text{Zn}_{1-x}\text{Mg}_x\text{O}$  and  $\text{Zn}_{1-y}\text{Cd}_y\text{O}$  thin films were firstly processed under air annealing. As displayed in Fig. 2a, the optical transmission spectra exhibit a high transmittance (about 80–90%) in visible region and a high absorption (near 100%) in UV region. The optical energy gap  $E_g$  for the direct electron transition can be determined using the following equation:

$$\alpha h\nu = C(h\nu - E_g)^{1/2} \quad (1)$$

where  $C$  is a constant,  $\alpha$  is the absorption coefficient and  $\nu$  is the photon frequency [27]. As shown in Fig. 2b, the fundamental absorption, which corresponds to the electron excitation from valance band to conduction band, is usually used to calculate the value of band gap using Eq. 1 by plotting the square of the optical absorption coefficient as a function of the photo energy and by extrapolating the linear region to the energy axis. The determined values are shown in the inset of Fig. 2b. The linear variation of band gap by Mg and Cd doping in ZAO further confirms that the Mg and Cd are doped into the matrix, which is consistent with our result of XRD study. However, the resistivity is out of the measurement range of our Hall effect system, this might be due to the insufficiency of carriers, such as oxygen vacancies ( $V_O$ ), which are decreased after air annealing. Therefore, we annealed these films under hydrogen (mixed with 95% argon) and vacuum ( $\sim 5 \times 10^{-2}$  Pa), respectively. After being treated in the hydrogen environment, the transmittances of (Cd, Al) codoped ZnO are heavily destroyed to  $\sim 30\%$

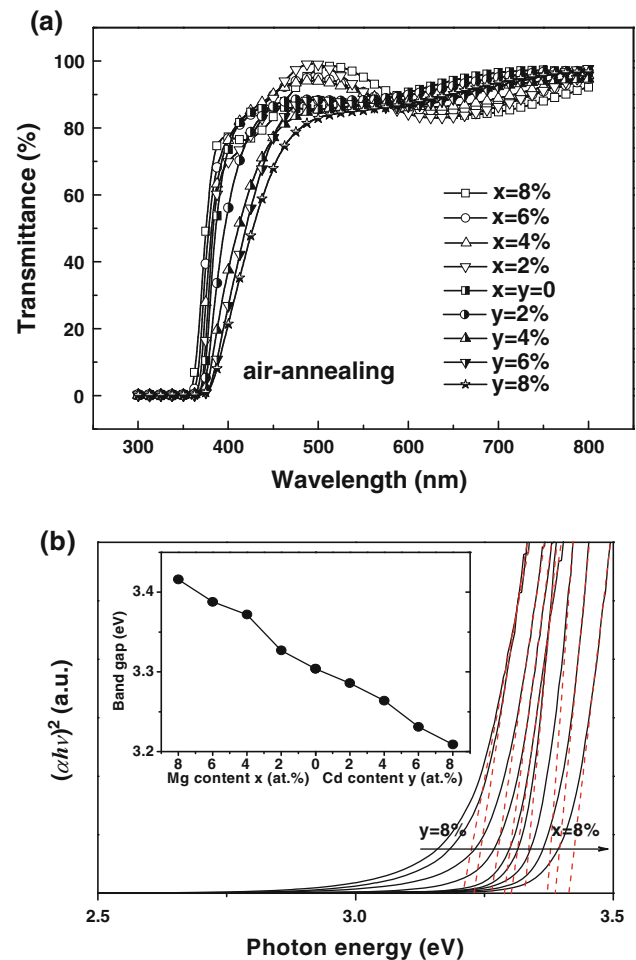


**Fig. 2** a Transmission spectra of 1 at.% Al-doped  $\text{Zn}_{1-x}\text{Mg}_x\text{O}$  and  $\text{Zn}_{1-y}\text{Cd}_y\text{O}$  films treated by air annealing. b Plot of square of the absorption coefficient versus photon energy for Al-doped  $\text{Zn}_{1-x}\text{Mg}_x\text{O}$  and  $\text{Zn}_{1-y}\text{Cd}_y\text{O}$  films. *Inset* the optical band gap energies as a function of Mg or Cd content

(not shown here), and the transmittances of vacuum treated films are obviously decreased to 50–60% as showed in Fig. 3a, comparing with the transmittance of air annealing films (80–90%). When the films annealed in vacuum, besides increasing the quantity of  $V_O$ , the deficiency of oxygen would degrade the crystallinity of the films due to the derivation of stoichiometry of ZnO matrix. Then, more lattice defects scattering might decrease the transmittance. The determined  $E_g$  after vacuum annealing is shown in the inset of Fig. 3b. The evolution of band gap by Mg and Cd codoping after vacuum annealing is almost same as that after air annealing. As a result, the Mg and Cd work effectively on band gap engineering, irrespective of the existence of Al codoping or annealing process. Even better than that, the electrical properties of the films treated in vacuum is well improved and could be measured by our Hall system, i.e. the resistivity has been reduced to the order of

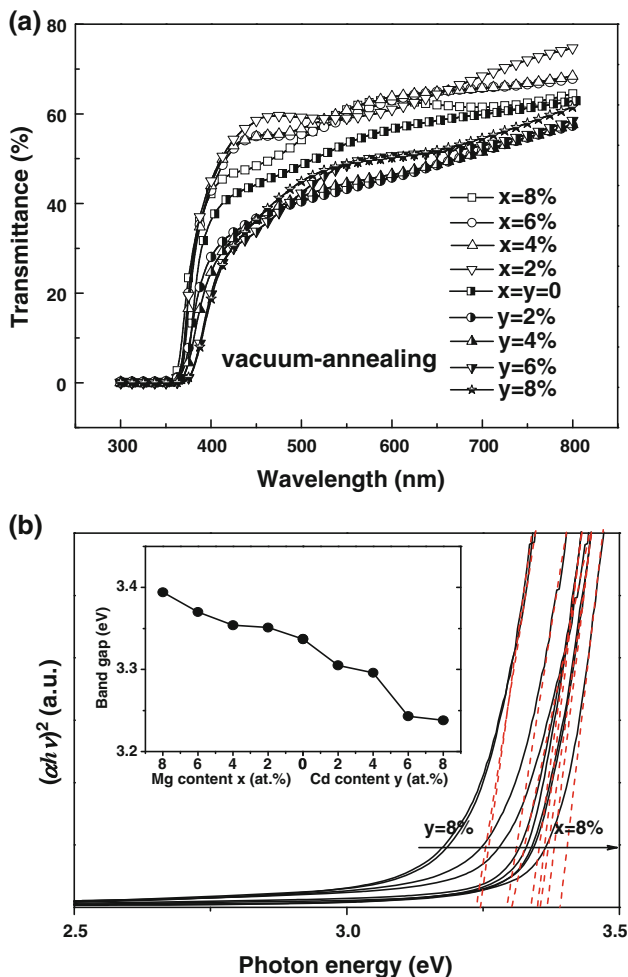


**Fig. 3** **a** Transmission spectra of 1 at.% Al-doped  $Zn_{1-x}Mg_xO$  and  $Zn_{1-y}Cd_yO$  films treated by vacuum annealing. **b** Plot of square of the absorption coefficient versus photon energy for Al-doped  $Zn_{1-x}Mg_xO$  and  $Zn_{1-y}Cd_yO$  films. *Inset* the optical band gap energies as a function of Mg or Cd content

$10^{-2} \Omega \text{ cm}$ . It is found that the relation between conductivity and transmittance of looks like a tradeoff; films with higher conductivity having lower transmittance.

As shown in Fig. 4, the resistivity totally decreases with Mg content  $x = 8\%$  to Cd content  $y = 8\%$ , while the carrier concentration and Hall mobility increase. It was found that the (Mg, Al) or (Cd, Al) codoped ZnO films with smaller band gap energies have larger carrier concentration and higher mobility. In Al-doped ZnO films studied by Lu et al. [7] and Nasr et al. [9], the initial increase in the band gap with Al doping (having higher carrier concentration) can be explained by the band gap widening phenomenon described by Burstein and Moss [28, 29]. The Fermi level in degenerate semiconductors is above the conduction band edge (due to partially-filled states in the conduction band), optical excitations from valence band to the Fermi level require an extra energy. It

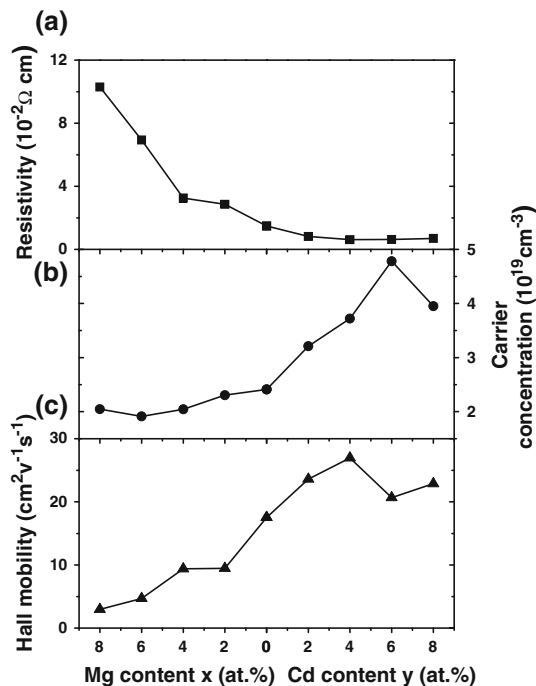


**Fig. 4** Resistivity (a), carrier concentration (b), and Hall mobility (c) of Al-doped  $Zn_{1-x}Mg_xO$  and  $Zn_{1-y}Cd_yO$  films

has been shown that this widening is a function of the carrier density according to the formula:

$$\Delta E_g = \frac{h^2}{8m_c^*} \left(\frac{3}{\pi}\right)^{2/3} n_c^{2/3} \quad (2)$$

where  $h$  is the Planck constant,  $m_c^*$  is the reduced effective mass, and  $n_c$  is the charge carrier concentration. At higher doping concentration of Al, the dopant atoms tend to segregate more and more at the grain boundaries, significantly increasing impurity scattering. The subsequent shrinkage of the band gap can be due to the electron impurity scattering as described by Hamberg et al. [30] In our (Cd, Al) or (Mg, Al) codoped ZnO films, as shown in Fig. 5, the dependence of band gap on carrier concentration is contrast to that of Al-doped ZnO [7, 9], which manifests that the underlying physical origin might be quite different.

Generally, there are several scattering mechanisms in the films, such as lattice vibration scattering, grain boundary scattering, ionized impurity scattering, neutral impurity scattering, etc., depending on the range of carrier concentration and the temperature of the films [7, 25]. In the present study, all the measurements of the conductive properties were collected at room temperature and the effect of lattice scattering which was determined by the variation of temperature could be ruled out. Within the framework of potential barrier model at grain boundaries [31, 32], defects located at grain boundaries can act as

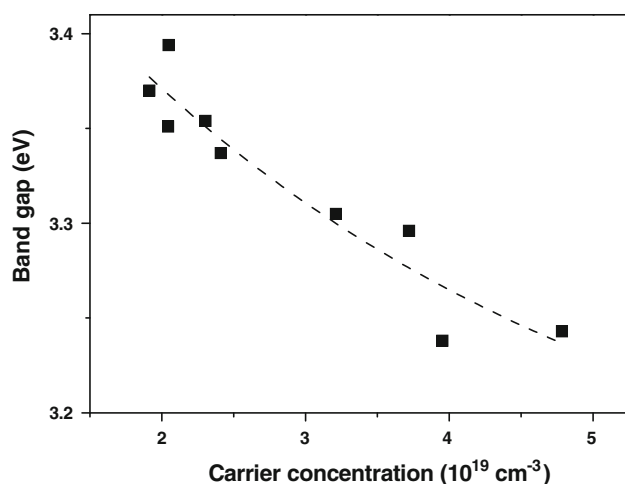


**Fig. 5** Dependence of band gap on carrier concentration of Al-doped  $\text{Zn}_{1-x}\text{Mg}_x\text{O}$  and  $\text{Zn}_{1-y}\text{Cd}_y\text{O}$  films

carrier traps and the trapped electrons set up a negative charge, contributing to rise to a space charge region in the grains. This will produce a potential barrier at the grain boundaries and decrease the Hall mobility of carriers. Zhu et al. [25] find that when the carrier concentration is low (approximately  $N \leq 5.0 \times 10^{18} \text{ cm}^{-3}$ ), grain boundary model is valid. However, the barrier height will decrease with the increase in carrier concentration, when the carrier concentration is high, the carrier tunneling current plays a more important role in the electrons transportation and the grain boundary scattering even can be neglected. The carrier concentrations of our codoping films are higher ( $>1.0 \times 10^{19} \text{ cm}^{-3}$ ), so the grain boundary scattering was tiny enough to be ignored. In this case, ionized impurity and natural scattering should make main contribution to the variation of the Hall mobility.

In Fig. 4, the resistivity increases with Mg content, while the carrier concentration and Hall mobility both decrease, which is consistent with the results of other groups for (Mg, Al)-codoped ZnO [2, 33, 34]. There might be two possible reasons for this phenomenon. Firstly, the incorporation of Mg introduces an extra impurity scattering, which could in turn decrease electron Hall mobility [2]. The second possibility is an increase in electron effective mass. Hall mobility can be defined using the following equation:

$$\mu = \frac{q\langle\tau\rangle}{m^*} \quad (3)$$

in which  $\langle\tau\rangle$  is the electron average scattering time and  $q$  is the electron charge. Films with a higher Mg content have higher electron effective mass values and lower mobility values [2]. And the decrease of carrier concentration indicates that the addition of Mg will lower the Al doping efficiency [2, 33]. Given the relatively lower carrier

concentration of the films, there would be more Al playing as scattering centers in reducing the electron mobility instead of providing carriers to the conduction band of the codoping films. Besides, the possible generation of more voids and pores observed by high-resolution field emission scanning electron microscope (FESEM) as Mg is incorporated, which adsorb oxygen and trap the free carriers, might also reduce the conductivity [16, 35].

On the other side, in thermal equilibrium, the electron concentration in conduction band ( $n_0$ ) and hole concentration ( $p_0$ ) in valence band has the relation,

$$n_0 p_0 = 4 \left( \frac{2\pi k}{h^2} \right)^3 (m_n^* m_p^*)^{3/2} T^3 \exp\left(-\frac{E_g}{kT}\right) \quad (4)$$

where  $h$  is the Planck constant,  $k$  is the Boltzmann constant,  $m_n^*$  and  $m_p^*$  is the electron and hole effective mass, respectively [36]. In ZnO-based thin films, the  $n$ -type carriers are dominant, as indicated in Fig. 5, the carrier concentration of our films increases with narrowing energy band, which is rather contrast the carrier concentration dependence of band gap shift in Al-doped ZnO films reported by Lu et al. [7, 9, 37], i.e. the Burstein-Moss Fermi-band filling effect is not suitable for our films. As the resistivity ( $\rho$ ) can be defined as

$$\rho = \frac{1}{\mu n q} \quad (5)$$

where  $\mu$  is mobility as defined in Eq. 3 and  $q$  is the electron charge [23], films with higher Cd content possess higher mobility and carrier concentration, and then lower resistivity. Actually, for Eq. 3, the effective mass of Cd is larger than that of Mg [38], so the electron average scattering time ( $\langle\tau\rangle$ ) of (Cd, Al) codoped ZnO might be shorter than that of (Mg, Al) codoped ZnO, due to the lattice expand of Cd doping, as shown in the inset of Fig. 1 and phonon dynamics study of Zn(Mg, Cd)O by Ghosh et al. [38] Based on the discussion above, band gap modification by Cd codoping in ZAO films might be a reasonable way to obtain high carrier concentration with simultaneous increasing mobility.

#### 4 Summary

$\text{Zn}_{1-x}\text{Mg}_x\text{O}:\text{Al}$  and  $\text{Zn}_{1-y}\text{Cd}_y\text{O}:\text{Al}$  thin films were prepared on glass substrate by sol-gel method. The 1 at% Al-doped ZnO film was band gap modified by Mg or Cd codoping. The effects of narrowing and widening band gap on the conductivity were simultaneously compared using optical and electrical measurements. The transmittances of these films are obviously decreased by vacuum annealing to 50–60%. Contrast to the evolution in Al-doped ZnO

films, the carrier concentration and Hall mobility both increase, while the resistivity decreases with narrowing band gap from Mg to Cd codoping, i.e. the conductivity of ZAO thin films could be enhanced using a simply band gap engineering by Cd codoping, which might be applied to obtain high carrier concentration with simultaneous increasing mobility.

**Acknowledgments** This work is financially supported by NPU Foundation for Fundamental Research (NPU-FFR-JC201017), Ph.D. Programs Foundation of Ministry of Education of China (Grant No. 20106102120051) and National Natural Science Foundation of China (Grant No. 50872112).

## References

- D.S. Ginley, C. Bright, MRS Bull. **25**, 15 (2000)
- K. Matsubara, H. Tampo, H. Shibata, A. Yamada, P. Fons, K. Iwata, S. Niki, Appl. Phys. Lett. **85**, 1374 (2004)
- T. Minami, MRS Bull. **25**, 38 (2000)
- M. Lorenz, E.M. Kaidashev, H. von Wenckstern, V. Riede, C. Bundesmann, D. Spemann, G. Benndorf, H. Hochmuth, A. Rahm, H.-C. Semmelhack, M. Grundmann, Solid-State Electron. **47**, 2205 (2003)
- Z.Z. Li, Z.Z. Chen, W. Huang, S.H. Chang, X.M. Ma, Appl. Surf. Sci. **257**, 8486 (2011)
- S.S. Lin, J.L. Huang, P. Šajgalik, Surf. Coat. Technol. **185**, 254 (2004)
- J.G. Lu, Z.Z. Ye, Y.J. Zeng, L.P. Zhu, L. Wang, J. Yuan, B.H. Zhao, Q.L. Liang, J. Appl. Phys. **100**, 073714 (2006)
- J. Mass, P. Bhattacharya, R.S. Katiyar, Mater. Sci. Eng. B **103**, 9 (2003)
- B. Nasr, S. Dasgupta, D. Wang, N. Mechau, R. Kruk, H. Hahn, J. Appl. Phys. **108**, 103721 (2010)
- T. Makino, Y. Segawa, M. Kawasaki, A. Ohtomo, R. Shiroki, K. Tamura, T. Yasuda, H. Koinuma, Appl. Phys. Lett. **78**, 1237 (2001)
- Z.Z. Ye, D.W. Ma, J.H. He, J.Y. Huang, B.H. Zhao, X.D. Luo, Z.Y. Xu, J. Cryst. Growth **256**, 78 (2003)
- K.T. Ramakrishna Reddy, P. Prathap, N. Revathi, A.S.N. Reddy, R.W. Miles, Thin Solid Films **518**, 1275 (2009)
- R. Ghosh, D. Basak, Appl. Surf. Sci. **255**, 7238 (2009)
- A. Ohtomo, M. Kawasaki, T. Koida, K. Masubuchi, H. Koinuma, Y. Sakurai, Y. Yoshida, T. Yasuda, Y. Segawa, Appl. Phys. Lett. **72**, 2466 (1998)
- W.I. Park, G.-C. Yi, H.M. Jang, Appl. Phys. Lett. **79**, 2022 (2001)
- R. Ghosh, D. Basak, J. Appl. Phys. **101**, 023507 (2007)
- K. Sakurai, T. Takagi, T. Kubo, D. Kajita, T. Tanabe, H. Takasu, S. Fujita, S. Fujita, J. Cryst. Growth **237–239**, 514 (2002)
- H.S. Kang, J.W. Kim, J.H. Kim, S.Y. Lee, Y. Li, J.-S. Lee, J.K. Lee, M.A. Nastasi, S.A. Crooker, Q.X. Jia, J. Appl. Phys. **99**, 066113 (2006)
- Th. Gruber, C. Kirchner, R. Kling, F. Reuss, A. Waag, F. Bertram, D. Forster, J. Christen, M. Schreck, Appl. Phys. Lett. **83**, 3290 (2003)
- J. Zúñiga-Pérez, V. Muñoz-Sanjosé, M. Lorenz, G. Benndorf, S. Heitsch, D. Spemann, M. Grundmann, J. Appl. Phys. **99**, 023514 (2006)
- J. Ishihara, A. Nakamura, S. Shigemori, T. Aoki, J. Temmyo, Appl. Phys. Lett. **89**, 091914 (2006)
- C. Yang, X.M. Li, X.D. Gao, X. Cao, R. Yang, Y.Z. Li, Solid State Commun. **151**, 264 (2011)
- W. Wei, C.M. Jin, J. Narayan, R.J. Narayan, Solid State Commun. **149**, 1670 (2009)
- H. Wang, Z. Huang, J.W. Xu, L. Yang, M.F. Ren, J. Mater. Sci. Mater. Electron. **21**, 1115 (2010)
- M.W. Zhu, J. Gong, C. Sun, J.H. Xia, X. Jiang, J. Appl. Phys. **104**, 073113 (2008)
- S.R. Meher, K.P. Biju, M.K. Jain, J. Sol-Gel. Sci. Technol. **52**, 228 (2009)
- P.K. Basu, *Theory of optical process in semiconductors* (Clarendon, Oxford, 1997), p. 87
- E. Burstein, Phys. Rev. **93**, 632 (1954)
- T.S. Moss, Proc. Phys. Soc. Lond. Sect. B **67**, 775 (1954)
- I. Hamberg, C.G. Granqvist, K.F. Berggren, B.E. Sernelius, L. Engström, Phys. Rev. B **30**, 3240 (1984)
- J. Bruneaux, H. Cachet, M. Froment, A. Messad, Thin Solid Films **197**, 129 (1991)
- V. Srikant, V. Sergo, D.R. Clarke, J. Am. Ceram. Soc. **78**, 1935 (1995)
- D.J. Cohen, K.C. Ruthe, S.A. Barnett, J. Appl. Phys. **96**, 459 (2004)
- G. Li, X.B. Zhu, X.W. Tang, W. Song, Z.R. Yang, J.M. Dai, J. Alloys Comp. **509**, 4816 (2011)
- S. Fujihara, C. Sasaki, T. Kimura, J. Euro. Ceram. Soc. **21**, 2109 (2001)
- E.K. Liu, B.S. Zhu, J.S. Luo, *Semiconductor physics* (National Defence Industry Press, Beijing, 1997), p. 58
- J.G. Lu, S. Fujita, T. Kawaharamura, H. Nishinaka, Y. Kamada, T. Ohshima, Z.Z. Ye, Y.J. Zeng, Y.Z. Zhang, L.P. Zhu, H.P. He, B.H. Zhao, J. Appl. Phys. **101**, 083705 (2007)
- M. Ghosh, N. Dilawar, A.K. Bandyopadhyay, A.K. Raychaudhuri, J. Appl. Phys. **106**, 084306 (2009)